

UNCLASSIFIED

AD NUMBER

AD016379

CLASSIFICATION CHANGES

TO: unclassified

FROM: confidential

LIMITATION CHANGES

TO:

Approved for public release, distribution unlimited

FROM:

Distribution authorized to U.S. Gov't. agencies and their contractors; Administrative/Operational use; 29 July 1953. Other requests shall be referred to Office of Naval Research, Arlington, VA 22217-0000.

AUTHORITY

ONR ltr, 18 May 1966; ONR ltr, 26 Oct 1977

THIS PAGE IS UNCLASSIFIED

UNCLASSIFIED

AD

16379

DEFENSE DOCUMENTATION CENTER

FOR

SCIENTIFIC AND TECHNICAL INFORMATION

CAMERON STATION ALEXANDRIA, VIRGINIA

CLASSIFICATION CHANGED

TO UNCLASSIFIED

FROM CONFIDENTIAL

PER AUTHORITY LISTED IN

DDI Form 129

1 July 1966



UNCLASSIFIED

INFLUENCE OF DENSITY AND INERT ADDITIVES ON THE
WAVE SHAPE OF "IDEAL" EXPLOSIVES

Investigators:

M. A. Cook
A. S. Filler
G. S. Horsley
S. D. Malstrom
D. W. Robinson
D. S. Partridge
W. S. Partridge
W. O. Ursenbach

Report Prepared by:

M. A. Cook
G. S. Horsley

M. A. Cook
Project Director

Technical Report No. XVII

July 29, 1953

Contract No. N7-onr-45107

Project No. 357 239

"THIS MATERIAL CONTAINS INFORMATION AFFECTING THE NATIONAL
DEFENSE OF THE UNITED STATES WITHIN THE MEANING OF THE
ESPIONAGE LAWS, TITLE 18, U. S. C., SECTIONS 793 AND 794
THE TRANSMISSION OR REVELATION OF WHICH IN ANY MANNER TO
AN UNAUTHORIZED PERSON IS PROHIBITED BY LAW."

Explosives Research Group
Institute for the Study of Rate Processes
University of Utah
Salt Lake City

CONFIDENTIAL

CONFIDENTIAL

Influence of Density and Inert Additives on the
Wave Shape of "Ideal" Explosives

Abstract

Wave shape-density measurements for "ideal" ($D = D^*$) TNT, pentolite, and various TNT-salt and pentolite-salt mixtures are reported. The radius of curvature/diameter (R/d) ratios at a charge length of six diameters were found to vary almost linearly with density. In TNT, however, a sharp discontinuity in the density- R/d curve occurred at a density of 1.35. This discontinuity was attributed to particle break-down during pressing at high densities.

Two additional series of R/d vs. charge length L measurements are reported, one for pure RDX and the other for 40-60 RDX-salt. In both instances R/L remained unity up to an L/d of 2.6. Between 2.6 and 4.6, R leveled off in both cases and reached the constant (steady state) value, remaining constant for higher values of L/d . This result is in agreement with previous observations that a steady state condition maintains for L/d values greater than about three.

R/d measurements were made for various TNT-salt, TNT-glass beads, RDX-salt, RDX-glass beads, and 50/50 pentolite-salt mixtures. R/d was found to decrease linearly with per cent inert for loose-packed TNT in 10 cm. diameter charges from about 2.1 with zero per cent salt to 1.3 with 60 per cent salt. In all other cases no definite trend in the R/d -per cent inert curves could be established, although if corrections for density were applied, R/d would be found to decrease with inert content in the cast TNT-salt, TNT-glass beads, and RDX-salt mixtures. In the pentolite-salt and RDX-glass bead series, R/d appeared to go through a maximum and then decrease with increasing inert content. However, erratic results, attributed to the combined effects of segregation, slowing down of the reaction rate, and attenuation of the wave toward the charge axis due to increased vaporization of the inert toward the central axis, made quantitative evaluations very difficult. The trends which were indicated in these latter cases are therefore open to doubt.

CONFIDENTIAL

CONFIDENTIAL

-2-

Introduction

Technical Report No. IX⁽¹⁾ under this project described some wave wave shape measurements in five explosives all with ideal or hydrodynamic velocities and in cylindrical charges. From that study it was concluded that the wave front was remarkably spherical in shape over almost the entire wave front except perhaps at the extreme edge despite the interesting fact that the radius of curvature at large length/diameter (L/d) ratios was much smaller than one would obtain for a spherically expanding wave front. Furthermore it was found that R increased only over the first few charge diameters after which it remained constant. Also the ratio R/d at L/d \approx 3-4 was relatively independent of charge diameter although there was a small increase in R/d in TNT and tetryl between 2.5 and 7.5 cm. diameters. The important observation was made, moreover, that the wave shape attained the same (steady state) value of R/d irrespective of the wave shape of the booster. This was clearly demonstrated by the fact that an initially re-entrant wave inverted completely to the steady state wave shape over a charge length of less than six diameters. It was also noted in initial studies that the wave shape depended critically on charge density.

More recent studies of wave shape in non-ideal explosives (T. R. XIV and XV)^(2,3) showed that even in the non-ideal explosives coarse TNT and amatol, the shape of the wave front remained spherical over practically the entire wave front, but the R/d ratio for L/d \approx 6.0 increased with diameter from about 0.5 at the critical diameter d_c to an asymptotic value about 1.9 for the coarse TNT and about 2.2 for cast 50-50 amatol above the minimum diameter d_m^* for attainment of the hydrodynamic velocity D^* . At diameters above d_m^* the R/d ratio apparently still depends to some extent on the density and chemical nature of the explosive since the R/d - d curve leveled off at a larger diameter than was the case with the D - d curves. Experimental measurements of the effects of density and chemical composition of R/d are therefore definitely needed in the development of an understanding of the principles determining wave shape.

CONFIDENTIAL

The influence of density on the wave shape of some ideal explosives have now been studied quantitatively. In addition, on the assumption that a study of the influence of inert additives would aid in an interpretation of wave shape in non-ideal explosives, several series of compositions with varying percentages of inert additives (salt and glass beads) were studied. Finally two more series of R vs. L measurements were made, one with pure granular RDX and the other with the granular 40 per cent RDX-60 per cent salt mixture. The results of these studies are presented in this report.

Material and Experimental Methods

The explosives used in this investigation were TNT, RDX, and 50-50 pentolite. The inert additives were NaCl (20-28 mesh) and glass beads (20-30 mesh). The most extensively studied explosive was pure TNT. In the first series, pure TNT was studied at various densities in 5.17 cm. diameter charges all of L/d approximately six. The lowest density charges in this series (densities .88 to .98) were vibrator-packed in manila paper tubes of about 1 mm wall thickness. To insure flat uniform ends for measurement of wave shape, thin glass plates were placed on the ends of the charges. The higher density charges (densities 1.08 to 1.53) were pressed in 5.17 cm. diameter and 2.6 cm. long wafers. Twelve such wafers were placed end to end and wrapped in paper with the bare end exposed for wave shape measurements. Similar pressed pellet charges were made with 70-30 TNT-salt, 40-60 TNT-salt, pure 50-50 pentolite, 70-30 pentolite (50-50)-salt and 40-60 pentolite (50-50)-salt compositions, pressing the charges in each case at low, intermediate, and high densities.

Vibrator-packed charges of 9.94 cm. diameter were made with pure RDX; 70-30 and 40-60 RDX-glass bead; pure TNT; 85-15, 70-30, 55-45, and 40-60 TNT-salt mixtures; and 80-20, 60-40 TNT-glass bead mixtures. In all of these charges, thin glass plates were placed on the end of the charge to provide a smooth, well-defined surface for photographing the

CONFIDENTIAL

-4-

emerging wave fronts. Finally cast charges of 90-10, 80-20, 70-30, 60-40, and 50-50 TNT-salt in 9.94 cm. diameter were made using smooth plastic on the end of the charge to form a smooth cast surface. These plastic plates were removed before firing, thus exposing the bare cast surface for wave shape measurements. In all cases, tube ends were cut on a lathe to insure that the end was exactly perpendicular to the charge axis.

The 5.17 cm. pressed charges were shot with pressed 5.17 cm. (d) x 2.6 cm. (L) tetryl boosters having a 1.9 cm. deep axially centered cap well. The loose-packed charges were point initiated with No. 8 EB caps axially centered by means of wooden forms. The cast charges were fired with axially centered 2" x 2" cast pentolite boosters in which were formed 1" deep cap wells.

The No. 8 EB caps were fired by means of the discharge (through a coaxial line) from a one μ f condenser charged to 3500-5000 volts. While there was a time lag of about 5 μ sec in these caps, it was sufficiently reproducible that no difficulty was encountered in synchronization. This is strikingly illustrated in figure 1 which is a smear photograph of a shot in which four parallel charges of 5.17 (d) x 31.2 (L) cm. pressed TNT (ρ_1 - 1.45 to 1.53) were fired simultaneously with the camera focussed on the ends of the charges away from the points of initiation. The static images were obtained by first opening wide the slit and taking a snap photograph (with the mirror at rest). The slit was then set at 5 mils and an (over-exposed) snap shot taken defining the field of view of the camera during detonation. The smear photograph was taken at a mirror speed of 700 r.p.s. (writing speed 4470 m/sec).

Wave shapes were measured in all cases by means of the "screamer" streak camera described in T. R. XII⁽⁴⁾, which during this investigation was modified by installing a new synchronizer similar to that built for the "crooner" but of improved design. The modifications were as follows: Three ranges were provided for the phantastron delay circuits to give much greater flexibility to the instrument. The unit now also provides

CONFIDENTIAL

CONFIDENTIAL

-5-

a circuit to test the firing cable for unseen damage. A surplus Dallmeyer telephoto lens f:6.3, 36" focal length was also installed to obtain 2-1/2 times greater magnification. A reversible electrically powered drive was constructed to focus this lens assembly. The camera shutter now has an auxiliary switch which permits one to open the shutter without activating the firing unit. There is now no lucite between the emulsion and rotating mirror as in the former design. Instead the film is held along the edges in a close fitting track and the curvature of the film holds it against the lucite back. In addition the wind from the rotating mirror helps keep it smooth. A light-tight film container was built in to permit opening the camera, with only the part of the film used to thread the film track being exposed. With the controls provided, it is now possible to wind the film and set the mirror for static images without opening the camera. The camera is synchronized at a predetermined time interval by means of the phantatron delay section; thus location of a trace is made possible at any desired position along the film. Generally the camera was operated at a mirror speed of 600 r.p.s. (3.83 mm/ μ sec before modification, 3.75 mm/ μ sec after modification), although in some cases speeds of 700 and 400 r.p.s. were used in an effort to obtain optimum definition depending on the velocity of the explosive and radius of curvature of the wave. To obtain more accurate results, especially for large R/d ratios in the highest velocity explosives, recently a smaller (1-1/2" x 3") mirror was installed making it possible to increase the mirror speed to about 800 r.p.s. The camera may now be operated at a writing speed up to 5 mm/ μ sec in wave shape measurements with explosives of high R/d ratio.

Velocities were measured by means of the "pansy" oscilloscope described in T. R. XI⁽⁵⁾, using, in the case of the cast and vibrator-packed charges, the regular pin assemblies described in T. R. XI. In the pressed charge, "pins" consisted of .001" brass foils placed between appropriate pellets using only a trigger and two time interval "pins".

To reduce the information on the photographs to useful form, the coordinates of various points along the trace were read using a Cambridge

CONFIDENTIAL

Universal Measuring Machine. These measured points were then corrected for magnification, camera writing speed and detonation velocity, and the data across a diameter of the charge plotted. These plots show the actual shape of the front of the detonation wave. A best fitting arc of a circle was then passed through the experimental points. In this work, as well as previous wave shape studies reported in T. R. IX, XIV, and XV, the only cases where the wave shape data could not be fitted satisfactorily with an arc of a circle over all but the edge of the wave was when the wave was obviously unsymmetrical, due most likely to some non-uniformity in the charge. At the extreme edge of the wave front the radius of curvature frequently was observed to fall off, especially in bare charges.

While the R/d results reported in this study were all obtained by the graphical method, D. W. Robinson has worked out an analytical procedure for obtaining the best fit of a circular arc which can be readily adapted to IBM calculations. This method, moreover, increases the accuracy of determination of wave shape. It is presented for its interest in future studies in Appendix I of this report.

Results

Tables I to VIII present the complete charge, density, and wave shape data determined in this study for the various mixtures. Velocity data were determined from the equation

$$D = D_{1,0} + S (\rho_1 - 1.0) \quad (1)$$

using the constants $D_{1,0}$ and S shown in table IX. These data were taken from OSRD 5611⁽⁶⁾ for TNT and RDX, and from data computed by the methods outlined in T. R. X⁽⁷⁾ for the explosive-salt mixtures. The velocities of the explosive-glass bead mixtures were not computed but were taken from experimental measurements. The data in table IX have all been carefully checked experimentally and found to be in excellent agreement with the observed velocities. A report showing this comparison and extending the developments outlined in T. R. X will be prepared in the near future.

The R/d vs. density data obtained for 100-0, 70-30, and 40-80 TNT-salt mixtures are plotted in figure 2. The limits of error are shown by means of the horizontal lines through the point designating the average value of R/d found from several measurements at each density. For pure TNT the reproducibility was good at densities up to 1.35. Above this value, however, the reproducibility was less satisfactory. This is associated partly with the difficulties in determining R/d accurately at large values of R, and partly to another factor perhaps associated with the interesting sudden increase in R/d as the density was increased above 1.35. The sharp break in the R/d vs. density curve at about 1.35 in density seems to be real since the limits of the experimental points do not overlap. One will note also that the value of R/d for pressed TNT is considerably greater than that for cast TNT described in T. R. IX at the same density. This is quite likely a particle size effect which is not eliminated even in "ideal" explosives. It is possible also that the discontinuity in the R/d-density curve at 1.35 in density is a particle size effect. One requires relatively small pressures to reach a density of 1.35 in pressed TNT. However, to obtain higher densities, the pressing force must be increased sharply. It is possible that the individual grains commence to rupture at the pressures required to go above 1.35 in density. The 70-30 and 40-60 TNT-salt mixtures gave R/d - ρ_1 curves approximately parallel to the pure TNT curve at low density. The pressing force required to attain the highest densities shown here were lower than that required to obtain a density of 1.4 with pure TNT. It may thus be for the reason that the pressing force was insufficient to cause grain break-down that there was no apparent tendency for the TNT-salt mixtures at the densities studied to show a plateau such as that observed with the pure TNT charges, although too few densities were studied to warrant conclusions on this point.

Figure 3 shows a plot of R/d vs. per cent TNT for the 9.94 cm. diameter vibrator-packed TNT-salt mixtures. R/d is shown to decrease approximately linearly with salt content. Similar measurements with cast

CONFIDENTIAL

-8-

TNT-salt mixtures, however, gave very erratic wave shape results. The irreproducibility in this case may be associated with segregation of salt during cooling of the cast mixture. Segregation of the TNT-salt mixtures would tend to slow down the wave toward the central axis relative to that on the periphery of the charge. This effect shows up as an increased radius of curvature along the central axis. It is believed therefore that the measured wave shapes in this case at least represent upper limits of R/d . Assuming this to be the case, it is probable that if segregation could be prevented, the R/d curve for cast TNT-salt mixtures would also decrease uniformly with salt content.

Incidentally, it was determined that the 25-75 vibrator-packed TNT-salt mixture detonated with a 2 x 2" cast pentolite booster, but failed with a cap. The 10-90 mixture, however, would not propagate. The fact that one obtains propagation with 75 per cent salt in TNT shows clearly that the salt acts primarily as an inert. Otherwise, the cooling effect of reacting salt would quench the detonation at a much lower percentage of salt.

With glass beads of nearly the same particle size as salt, there was apparently no change of R/d with per cent inert in the TNT-glass beads series. However, if a correction were made for density, the effect of inert would again be found to decrease the R/d ratio. Similar results with the RDX-salt mixtures are shown in table VII. However, with the vibrator-packed RDX-glass beads mixtures, R/d appeared to increase sharply with per cent inert, and was still greater in the 40-60 RDX-glass beads mixture than in pure RDX (table VIII). It was considered that this effect might also be due to segregation. This explanation was supported by the fact that in pressed TNT-salt mixtures, the expected decrease in R/d with per cent inert was observed and the further fact that results with the pressed charges were fairly reproducible. Before accepting this explanation, however, a series of pressed 50-50 pentolite-salt mixtures were studied in which segregation was, of course, not possible. The results are given in table VI and plotted in figure 4. The R/d -density-

CONFIDENTIAL

CONFIDENTIAL

-9-

curve for pure 50-50 pentolite appears comparable to that of pure TNT at low density except that R/d was somewhat larger at a given density. Moreover the results of two check determinations were in good agreement. However, for the pentolite-salt mixtures results were again poorly reproducible and showed the same trends as with RDX-glass beads. That is, the 30 per cent inert mixture had even less curvature at a given density than for pure pentolite although the 40-60 mixture showed a lower R/d , indicating that the R/d -per cent inert curve at a given density may pass through a maximum in this case. However, this conclusion is indefinite since the differences were of the same order of magnitude as the experimental error.

A striking result with the pressed pentolite-salt mixtures was the fact that despite the impossibility for segregation, the waves frequently were found to be asymmetrical about the charge axis. In order that these effects might be available for careful study, the experimental data that were used to make the wave shape plots in this investigation are given in Table X. It seems quite possible, in view of asymmetrical conditions, and the poor reproducibility of wave shapes obtained with the various explosive-inert mixtures, that erratic (apparently wobbling) waves may be a characteristic of such mixtures. This would explain also the fact that the reproducibility of velocity determinations invariably decreases with increasing inert content in explosives of this character.

As in the explosive-salt and glass beads mixtures, one experiences the same type difficulties of irreproducibility, wave asymmetry and flattening out of the wave toward the central axis with aluminized explosives including 20-80 tritonal and 25-75 Al-composition B. This seems clearly to be a segregation effect in aluminized explosives. It is very difficult to obtain cast charges in these explosives in which no segregation of aluminum occurs.

The variation of R/d with charge length for pure granular RDX and 40-60 RDX-salt mixture is shown in table VII. For pure RDX, R/L was unity within very close limits for values of L/d up to 2.6. For L/d

CONFIDENTIAL

CONFIDENTIAL

-10-

between 3.0 and 4.5, R continued to increase, but at a rapidly decreasing rate reaching a constant value of 3.5 d above an L/d of 4.5. In 40-60 RDX-salt mixtures, R/L again remained at unity up to an L/d of 2.6. Again R appeared to reach a constant value somewhere between an L/d of 2.6 remaining constant for values of L/d of 4.6 and greater. It is evidently not possible within the limits of experimental error to distinguish between the different explosives as far as the determination of the minimum value of L/d for attainment of the steady state wave curvature is concerned. This is in agreement with results found in studies of the influence of charge length on shaped charge results. In those studies optimum shaped charge effect with unconfined charges was also found to be reached at an L/d between about 2.5 and 4.5. Similar results were obtained with confined charges.

Discussion of Results

Wave shape even in ideal explosives depends not only on the chemical nature of the explosive but also on its physical state. The influence of physical state is strikingly illustrated in a comparison of cast and pressed TNT. In cast TNT at a density of 1.59 in 7.5 cm. diameter charges of L/d = 6, a value of 2.4 for R/d was obtained. However, for the 5.17 cm. (d) pressed charges at slightly lower density (1.53), R/d was 4.6. One obvious difference between the cast and pressed TNT is particle size. The cast charges of R/d = 2.4 were not "creamed" but were poured cloudy. The effective particle size and reaction zone length a_0 in this material as shown in T. R. XV is greater than in the "creamed" product. The R/d in a pressed charge should be even less than in the "creamed" cast charge especially under the possibility that pressing at high densities reduces even further the particle size.

Effects of particle size on R/d for "ideal" explosives can be readily interpreted on the basis of the detonation head theory. According to this theory, D/D^* should be unity for all values of reaction zone length a_0 less than about d. For values of a_0 near d, however, only the explosive

CONFIDENTIAL

CONFIDENTIAL

-11-

along the central axis of the charge reacts completely within the detonation head. The wave would thus be attenuated toward the periphery of the charge which should lead to relatively large curvature or small R/d . For smaller values of a_0 the periphery attenuation would be less and the R/d correspondingly greater. A report presenting a theory of wave shape based on detonation head concepts will be presented in the near future.

R/d appears always to increase with charge density. In pressed TNT the R/d vs. ρ_1 curve was almost linear, the curve bending slightly toward larger R/d ratios at increased densities. This was true also for the explosives 70-30 and 40-60 TNT-salt, and 50-50 pentolite. The 70-30 and 40-60 pentolite-salt pressed charges showed a similar trend. Moreover, the slopes of the R/d vs. ρ_1 curves were comparable for all of these explosives. However, only in the cases of pure TNT, pure pentolite, and the TNT-salt mixtures are these results considered entirely reliable.

Since "creamed" cast TNT should have an effective particle size only slightly greater than that of the granular TNT from which it was made, an R/d of about 3.0 is predicted for the "creamed" cast TNT, on the assumption that the break in the R/d - ρ_1 curve was a particle break-down effect. That is, if particle break-down had not occurred, R/d should continue to increase almost linearly.

The results obtained with inert additives leave much to be desired. It was hoped by this study to obtain information which would aid in interpreting wave shape data for "non-ideal" explosive. That is, the part of the explosive which has not reacted within the detonation head might be considered to exert the same effect on wave shape as an inert. There are three possible factors, however, which might complicate this situation and render impossible the use of inert additives for this purpose. Firstly, segregation of the inert additive which is difficult to avoid tends to distort the wave from its true form due to attenuation of the wave in the region of high concentrations of the inert. Secondly, endothermic reaction of the inert if it takes place tends to slow down the rate of reaction of the explosive and thus increase the reaction zone length

CONFIDENTIAL

CONFIDENTIAL

-12-

a_0 , and decrease R/d . While the evidence from velocity measurements seems to show that reaction of NaCl in these explosive is relatively small if not negligible, since explosives reactions are surface reactions, it is possible that such inert additives as salt would tend to retard the reaction somewhat. Thirdly, even if retardation of the explosive reaction rate by the inert were negligible, one would expect a greater effective vaporation and resultant cooling effect along the central axis than toward the periphery of the charge because of the longer effective time for reaction along this axis than toward the periphery of the charge. This effect would tend to reduce wave curvature and increase R/d . Low density TNT is a much lower temperature explosive than pentolite and RDX. One might thus expect less vaporization of NaCl in the detonation head for TNT than for pentolite and RDX. Hence, in loose-packed TNT one may perhaps be observing the true dilution effect. The detonation temperatures of cast TNT, pentolite and RDX are enough higher that enough vaporation of NaCl may take place to cause the effects shown.

BIBLIOGRAPHY

1. Technical Report No. IX, this project, February 13, 1953 (Confidential)
2. Technical Report No. XIV, this project, June 10, 1953 (Confidential)
3. Technical Report No. XV, this project, July 3, 1953 (Confidential)
4. Technical Report No. XII, this project, April 30, 1953 (Confidential)
5. Technical Report No. XI, this project, April 5, 1953 (Confidential)
6. OSRD Report No. 5611
7. Technical Report No. X, this project, March 25, 1953 (Confidential)

CONFIDENTIAL

TABLE I: Wave Shape vs. Density Measurements for TNT
in 5.17 cm. Diameter Cylindrical Charges

Film No.	L Length (cm.)	ρ_1	D (m/sec)	R (cm.)	R/d	R/d (av.)
631	30.0	.878	4,620	8.9	1.7	1.7
632	30.0	.894	4,670	8.7	1.7	
615	29	.982	4,950	8.9	1.7	1.9
616	29	.982	4,950	9.3	1.8	
617	27	.982	4,950	10.4	2.0	
618	27	.982	4,950	10.1	1.9	
604	31.2	1.078	5,260	10.6	1.9	
605	31.2	1.078	5,260	10.5	1.9	1.9
606	31.2	1.170	5,560	11.4	2.2	2.3
608	31.2	1.170	5,560	11.5	2.2	
756	31.2	1.191	5,630	12.2	2.4	
757	31.2	1.191	5,630	11.5	2.2	
758	31.2	1.288	5,940	13.4	2.6	
761	31.2	1.288	5,940	12.5	2.4	2.5
602	31.2	1.354	6,150	13.4	2.6	2.8
603	31.2	1.354	6,150	14.2	2.7	
635	31.2	1.354	6,150	16.7	3.2	
759	31.2	1.368	6,200	16.9	3.3	3.1
760	31.2	1.366	6,190	15.1	2.9	
966	31.2	1.376	6,220	17.6	3.4	3.5
967	31.2	1.375	6,220	18.0	3.5	
968	31.2	1.423	6,370	22.3	4.3	4.0
969	31.2	1.423	6,360	18.7	3.6	
609	31.2	1.440	6,430	19.7	3.8	4.1
610	31.2	1.440	6,430	22.2	4.3	
984	31.2	1.469	6,520	23.1	4.5	4.3
985	31.2	1.471	6,530	21.3	4.1	
986	31.2	1.533	6,730	22.3	4.3	4.6
987	31.2	1.534	6,730	24.8	4.8	

CONFIDENTIAL

-14-

TABLE II: Wave Shape-Density Measurements for Pressed TNT-Salt (20-28 mesh) Mixtures in 5.17 cm. Diameter Cylindrical Charges

Film No.	L Length (cm.)	ρ_1	D (m/sec)	R (cm.)	R/d	R/d (av.)
70 per cent TNT 30 per cent salt						
1105	29.2	1.209	4,690	9.1	1.8	1.7
1110	29.2	1.207	4,690	8.3	1.6	
1106	29.4	1.351	5,230	10.9	2.1	2.0
1107	29.4	1.351	5,230	10.0	1.9	
1108	29.6	1.493	5,760	13.7	2.6	2.9
1109	29.6	1.492	5,760	16.3	3.2	
40 per cent TNT 60 per cent salt						
1111	29.2	1.361	3,880	4.2	0.8	0.8
1035	29.3	1.508	4,760	6.5	1.3	1.3
1114	29.3	1.508	4,500	6.0	1.2	
1030b	29.4	1.649	5,040	9.3	1.8	1.8
1122	29.5	1.642	5,110	8.7	1.7	

CONFIDENTIAL

TABLE III: Wave Shape Measurements for Vibrator-Facked TNT and TNT-Salt Mixtures in 9.94 cm. Diameter Cylindrical Charges

Film No.	L Length (cm.)	ρ_1	D (m/sec)	R (cm.)	R/d	R/d (sv.)
100 per cent TNT						
518	60.85	.844	4,670	29.7	2.5	
569	60.8	.898	4,680	21.9	2.2	
954	59.4	.859	4,560	19.1	1.9	2.1
953	59.8	.855	4,540	18.6	1.9	
85 per cent TNT 15 per cent Salt						
664	60.9	.959	4,270	19.3	1.9	
766	61.0	.943	4,220	16.8	1.7	
767	61.0	.929	4,170	17.9	1.8	1.9
959	59.5	.949	4,240	20.5	2.1	
960	60	.939	4,210	20.6	2.1	
70 per cent TNT 30 per cent Salt						
581	60.85	1.010	3,950	18.0	1.8	
582	60.8	1.006	3,930	16.8	1.7	
589	60.8	.993	3,880	18.9	1.9	1.8
955	60.2	.993	3,880	17.5	1.8	
956	60.5	.991	3,880	17.6	1.8	
55 per cent TNT 45 per cent Salt						
703	59.0	1.067	3,440	16.6	1.7	
705	59.5	1.033	3,330	13.9	1.4	
706	60.9	1.089	3,530	13.9	1.4	1.5
708	60.9	1.115	3,630	13.7	1.4	
40 per cent TNT 60 per cent Salt						
586	60.85	1.140	3,000	11.7	1.2	
587	60.85	1.137	2,990	12.1	1.2	1.3
958	59.5	1.134	3,040	14.6	1.5	

TABLE IV: Wave Shape Measurements for Cast TNT-Salt
Mixtures in 9.94 cm. Diameter Cylindrical Charges

Film No.	L Length (cm.)	ρ_1	D (m/sec)	R (cm.)	R/d	λ/d (av.)
90 per cent TNT 10 per cent Salt (20-28)						
449	52.5	1.649	6,675	24.1	2.4	2.4
80 per cent TNT 20 per cent Salt (20-28)						
408	56	1.668	6,650	30.2	3.0	2.65
451	54.3	1.673	6,650	22.6	2.3	
70 per cent TNT 30 per cent Salt (20-28)						
405	56.6	1.672	6,380	15.8	1.6	1.6
60 per cent TNT 40 per cent Salt (20-28)						
403	56.1	1.730	6,173	21.7	2.2	2.4
444	53.2	1.756	6,835	19.7	2.0	
979	52.9	1.782	6,530	28.5	2.9	
980	62.7	1.788	6,550	25.3	2.6	
50 per cent TNT 50 per cent Salt (20-28)						
407	57.3	1.725	5,840	16.7	1.7	2.2
975	62.9	1.826	6,260	25.4	2.6	
976	62.8	1.828	6,270	21.8	2.2	

CONFIDENTIAL

-17-

TABLE V: Wave Shape Measurements for Vibrator-Packed
TNT-Glass Bead (20-30 mesh) Charges in 9.94 cm. Diameter Cylindrical Charges

Film No.	L Length (cm.)	ρ_1	D (m/sec)	R (cm.)	R/d	R/d (av.)
			80 per cent TNT	20 per cent Glass Beads		
685	59.5	1.055	4300	21.6	2.2	
731	61.8	.997	4200	21.9	2.2	2.2
			60 per cent TNT	40 per cent Glass Beads		
732	60.9	1.161	3800	24.0	2.4	
733	60.9	1.169	3800	21.0	2.1	2.3
			40 per cent TNT	60 per cent Glass Beads		
740	61.0	1.343	3320	20.4	2.1	2.1

CONFIDENTIAL

CONFIDENTIAL

-18-

TABLE VI: Wave Shape-Density Measurements for Pressed 50-50 Pentolite-Salt (20-28 mesh) Mixtures in 5.17 cm. Diameter Cylindrical Charges

Film No.	L Length (cm.)	ρ_1	D (m/sec)	R (cm.)	R/d
100 per cent pentolite					
1019	29.5	1.195	6,080	10.4	2.0
1020	29.6	1.341	6,540	15.7	3.0
1021	29.6	1.341	6,540	16.5	3.2
1030a	29.7	1.487	6,990	17.3	3.3
1022	29.7	1.487	6,990	19.3	3.7
70 per cent Pentolite 30 per cent Salt (20-28)					
1024	29.3	1.351	5,600	16.3	3.2
1025	29.3	1.356	5,600	14.5	2.8
1026	29.4	1.501	6,180	30.7	5.9
1027	29.4	1.503	6,040	21.9	4.2
1028	29.6	1.688	6,790	27.7	5.4
1112	29.6	1.681	6,750	21.8	4.2
40 per cent Pentolite 60 per cent Salt (20-28)					
1168	29.2	1.361	4,380	8.4	1.6
1169	29.1	1.361	4,380	11.1	2.1
1113	29.2	1.517	4,850	20.3	3.9
1167	29.2	1.518	4,940	13.2	2.6
1123	29.4	1.703	5,800	15.3	3.0

CONFIDENTIAL

CONFIDENTIAL

-19-

TABLE VII: Wave Shape Measurements for Granular (Vibrator-Packed) and RDX-Salt (20-28 Mesh) Mixtures in 9.94 cm. Diameter Cylindrical Charges at Various L/d Ratios

Film No.	L Length (cm.)	ρ_1	D (m/sec)	R (cm.)	L/d	R/d	R/d (ave.)
455	5.1	1.129	6,540	6.3	.51	0.6	
456	5.0	1.206	6,820	5.7	.5	0.6	.6
458	7.7	1.203	6,810	8.5	.77	0.9	.9
457	10.1	1.177	6,720	9.3	1.0	0.9	
459	10.1	1.253	6,990	9.7	1.0	1.0	1.0
461	15.2	1.230	6,910	17.0	1.5	1.7	
462	15.2	1.230	6,910	16.2	1.5	1.6	1.7
463	20.3	1.195	6,780	20.2	2.0	2.0	
464	21.4	1.127	6,540	26.9	2.1	2.7	2.4
465	26	1.175	6,710	26.7	2.6	2.7	
466	25.5	1.203	6,810	24.7	2.6	2.5	2.6
576	30.4	1.215	6,670	25.6	3.0	2.6	
619	30.2	1.169	6,500	24.5	3.0	2.5	
620	30.4	1.184	6,560	27.9	3.0	2.8	2.7
678	30.5	1.203	6,620	26.4	3.1	2.7	
679	30.4	1.180	6,540	26.5	3.0	2.7	
675	42.3	1.264	6,840	29.8	4.2	3.0	3.0
577	45.6	1.234	6,740	31.5	4.6	3.2	
624	45.3	1.254	6,810	33.5	4.5	3.4	3.5
674	45.2	1.220	6,690	38.3	4.5	3.9	
475	58.2	1.168	6,680	34.1	5.8	3.4	
478	56.0	1.214	6,850	36.7	5.6	3.7	
479	55.4	1.266	7,030	33.5	5.5	3.4	3.5
592	60.8	1.230	6,720	34.5	6.1	3.5	

40 per cent RDX 60 per cent Salt (20-28)

484	2.6	1.4	4,700	2.4	.26	.24	.24
-----	-----	-----	-------	-----	-----	-----	-----

CONFIDENTIAL

CONFIDENTIAL

-20-

TABLE VII (cont'd)

Film No.	L Length (cm.)	ρ_1	D (m/sec)	R (cm.)	L/d	R/d	R/d (ave.)
485	5.10	1.432	4,700	5.9	.51	0.6	.61
486	5.10	1.432	4,700	6.2	.51	0.6	
487	7.7	1.423	4,600	9.4	.77	0.9	.94
488	10.2	1.432	4,700	12.0	1.0	1.2	1.2
489	10.2	1.432	4,700	12.2	1.0	1.2	
490	15.2	1.562	5,280	20.1	1.5	2.0	2.0
491	15.3	1.562	5,280	20.3	1.5	2.0	
492	20.3	1.566	5,300	18.0	2.0	1.8	2.0
493	20.3	1.566	5,300	25.4	2.0	2.6	
682	20.4	1.489	4,990	16.9	2.0	1.7	
494	25.6	1.548	5,220	20.7	2.6	2.1	2.1
572	25.5	1.526	5,120	20.5	2.6	2.1	
499	30.6	1.516	5,070	33.6	3.1	3.4	2.4
621	30.4	1.525	5,110	15.8	3.0	1.6	
681	30.6	1.532	5,140	20.8	3.1	2.1	
579	45.5	1.500	5,000	33.8	4.6	3.4	3.2
580	45.8	1.520	5,090	29.7	4.6	3.0	
476	55.8	1.539	5,180	26.5	5.6	2.7	3.3
590	60.8	1.502	5,010	38.1	6.1	3.8	
593	60.8	1.532	5,040	36.6	6.1	3.7	
594	60.9	1.502	5,010	41.8	6.1	4.2	
686	61.2	1.520	5,090	27.3	6.1	2.7	
687	61.1	1.513	5,010	27.6	6.1	2.8	

70 per cent RDX 30 per cent Salt

473	60.8	1.334	5,760	39.7		4.0	3.5
480	58.0	1.329	5,410	29.4		3.0	
481	60.2	1.365	5,910	35.8		3.6	
626	59.9	1.342	5,800	28.4		2.9	
627	60.5	1.357	5,850	39.2		3.9	
628	60.2	1.372	5,950	35.9		3.6	
688	60.6	1.355	5,830	37.1		3.7	
689	60.7	1.359	5,850	33.3		3.3	

CONFIDENTIAL

CONFIDENTIAL

-21-

TABLE VIII: Wave Shape Measurements for
Granular (Vibrator-Packed) RDX-Glass Bead Mixtures in 9.94 cm.
Diameter Cylindrical Charges

Film No.	L Length (cm.)	ρ_1	D (m/sec)	R (cm.)	R/d	R/d (av.)
80 per cent RDX 20 per cent Glass (20-30)						
739	60.8	1.340	6,150	44.7	4.5	4.7
741	60.9	1.334	6,150	49.0	4.9	
40 per cent RDX 60 per cent Glass (20-30)						
917	61.0	1.522	5,100	33.3	3.3	3.9
918	61.0	1.506	5,100	43.7	4.4	

TABLE IX: Detonation Velocity-Density for Explosive-Salt Mixtures

$$D = D_{1.0} + S (\Delta_1 - 1.0)$$

Explosive	N_w	$D_{1.0}$	S
TNT	1.00	5010	3225
	0.90	4710	3265
	0.80	4405	3330
	0.70	4050	3435
	0.60	3610	3610
	0.50	3070	3840
	0.40	2415	4145
50-50 Pentolite	1.00	5480	3100
	0.80	4940	3120
	0.70	4600	3190
	0.54	3885	3420
	0.40	3070	3735
RDX	1.00	5900	3570
	0.70	4935	3095
	0.40	3300	3535
	0.20	1730	4180

CONFIDENTIAL

589

y(mm)	x(mm)
0.00	0.00
1.59	6.33
3.11	12.67
4.07	19.00
4.87	25.33
5.52	31.67
6.02	38.00
6.25	44.33
6.25	50.66
6.20	57.00
5.90	63.33
5.38	69.66
4.60	76.00
3.69	82.33
2.20	88.66

956 cont.

y(mm)	x(mm)
5.11	16.90
6.01	22.54
6.64	28.17
7.18	33.80
7.51	39.44
7.72	45.07
7.74	50.71
7.63	56.34
7.39	61.97
6.95	67.61
6.35	73.24
5.53	78.88
4.41	84.51
2.95	90.14
2.02	92.96
1.15	95.16

705 cont.

y(mm)	x(mm)
9.84	47.71
9.94	52.21
9.81	56.71
9.53	61.21
8.56	70.21
6.86	79.21
5.57	83.71
4.06	88.21
2.25	92.71
0.05	97.21

708 cont.

y(mm)	x(mm)
4.31	85.21
3.00	89.69
1.24	94.18
0.13	96.15

958 cont.

y(mm)	x(mm)
5.60	11.25
7.06	16.88
8.22	22.50
8.77	28.13
9.35	33.76
9.60	39.38
9.72	45.01
9.72	50.63
9.60	56.26
9.31	61.89
8.77	67.51
8.04	73.14
7.24	78.76
6.05	84.39
4.50	90.02
3.34	92.83
2.14	96.09

586

y(mm)	x(mm)
0.00	0.00
3.21	6.36
5.64	12.72
7.55	19.08
9.18	25.44
10.40	31.80
11.34	38.16
11.73	44.52
11.89	50.88
11.75	57.24
11.53	63.60
10.51	69.96
9.24	76.32
7.86	81.54

706

y(mm)	x(mm)
0.00	0.00
2.14	4.49
3.69	8.97
6.16	17.94
7.62	26.91
8.64	35.88
8.78	40.36
8.84	44.85
8.75	49.33
8.51	53.81
7.72	62.78
6.46	71.75
4.68	80.72
3.52	85.21
2.17	89.69
0.69	93.10

587

y(mm)	x(mm)
0.00	0.00
2.91	6.36
5.26	12.72
7.20	19.07
8.79	25.43
9.73	31.79
10.40	38.15
10.87	44.51
10.95	50.86
10.73	57.22
10.31	63.58
9.48	69.94
8.29	76.30
6.83	82.65
4.86	89.01
2.59	95.37
0.09	98.99

708

y(mm)	x(mm)
0.00	0.00
2.42	4.49
4.36	8.96
6.00	13.45
7.19	17.94
8.46	26.91
9.17	35.88
9.40	40.36
9.49	44.85
9.56	49.33
9.47	53.81
9.23	58.30
8.85	62.79
7.34	71.75
5.45	80.72

449

y(mm)	x(mm)
0.00	0.00
1.65	6.17
3.43	12.34
4.40	18.51
5.28	24.68
5.76	30.85
5.93	37.02
5.93	43.19
5.93	49.36
5.68	55.53
5.45	61.70
5.10	67.87
4.58	74.04
3.90	80.21
2.72	86.38
.85	92.55
-2.23	98.72
-2.40	99.87

955

y(mm)	x(mm)
0.20	0.00
1.71	2.84
2.68	5.68
4.10	11.36
5.34	17.05
6.28	22.73
7.06	28.41
7.50	34.09
7.80	39.77
7.97	45.46
7.97	51.14
7.89	56.82
7.62	62.50
7.07	68.18
6.38	73.87
5.54	79.55
4.53	85.23
3.15	90.91
2.36	93.75
1.41	96.59
0.00	99.21

703

y(mm)	x(mm)
0.84	0.00
1.94	2.34
3.38	6.84
5.16	15.84
6.48	24.84
7.40	33.84
7.67	38.34
7.76	42.85
7.82	47.35
7.78	51.85
7.64	56.35
7.43	60.85
6.76	69.85
5.54	78.85
4.53	83.35
3.28	87.85
1.69	92.35
0.00	96.22

705

y(mm)	x(mm)
0.00	0.00
1.78	2.70
3.78	7.20
6.32	16.20
7.99	25.20
9.04	34.20
9.70	43.21

956

y(mm)	x(mm)
0.00	0.00
1.75	2.42
2.73	5.63
3.96	11.27

958

y(mm)	x(mm)
0.00	0.00
2.26	2.81
3.60	5.63

408

y(mm)	x(mm)
0.00	0.00
1.30	8.75
2.03	17.51
2.55	26.26
3.14	35.01
3.47	43.77

459 cont.

13.67	40.25
13.72	46.96
13.65	53.66
13.05	60.37
11.97	67.08
10.22	73.79
8.43	80.50
5.95	87.20
2.77	93.91
0.00	99.41

463 cont.

1.12	55.33
3.51	15.99
4.90	26.65
5.89	37.31
6.32	47.97
6.35	53.30
6.44	58.63
5.33	69.29
3.97	79.95
2.30	90.61
0.04	99.41

466 cont.

2.35	10.74
4.07	21.48
5.21	32.22
5.85	42.96
6.13	48.33
6.01	53.70
5.85	64.44
4.98	75.18
3.70	85.92
2.38	96.66
1.97	99.40

620

y(mm)	x(mm)
0.00	0.00
1.23	4.15
1.97	8.30
3.02	16.60
3.82	24.90
4.47	33.20
4.88	41.50
4.97	49.80
4.93	58.10
4.59	66.40
4.06	74.70
3.26	83.00
2.21	91.30
1.53	95.45
0.75	99.60
0.29	101.76

679 cont.

1.52	92.94
0.43	98.02

675

y(mm)	x(mm)
0.57	0.00
1.45	4.16
2.02	8.32
3.00	16.63
3.68	24.95
4.18	33.26
4.48	41.58
4.48	49.90
4.30	58.21
3.89	66.53
3.32	74.84
2.52	83.16
2.05	87.32
1.45	91.48
0.77	95.63
0.00	98.88

461

y(mm)	x(mm)
0.34	0.00
1.91	5.50
3.41	10.99
5.02	21.98
6.28	32.97
7.51	43.96
7.90	49.46
7.85	54.95
2.13	65.94
5.03	76.93
2.76	87.92
0.00	99.41

464

y(mm)	x(mm)
0.00	0.00
0.70	5.49
2.51	16.47
3.74	27.45
4.51	38.42
4.60	49.40
4.77	54.89
4.68	60.38
4.13	71.36
3.31	82.34
1.28	93.31
0.29	99.41

576

y(mm)	x(mm)
2.63	0.00
3.26	3.91
4.01	10.54
5.35	23.79
5.73	30.42
5.91	37.04
5.91	50.30
5.49	56.92
4.84	63.55
3.75	76.80
2.79	83.43
1.71	90.06
0.00	96.68

678

y(mm)	x(mm)
0.54	0.00
1.97	6.20
2.90	12.39
4.27	24.78
5.06	37.18
5.18	43.37
5.12	49.57
4.98	55.77
4.68	61.96
3.70	74.35
2.30	86.74
1.35	92.94
0.00	99.14

577

y(mm)	x(mm)
1.29	0.00
1.97	6.37
3.17	19.11
3.40	25.48
3.57	31.85
3.52	44.59
3.29	50.96
2.99	57.33
2.25	70.06
1.78	76.43
1.04	82.80
0.00	89.17

462

y(mm)	x(mm)
0.00	0.00
0.96	5.34
2.33	10.68
5.16	21.35
6.77	32.03
7.43	42.70
7.70	48.04
7.88	53.38
7.70	58.72
7.43	64.06
6.55	74.73
4.13	85.41
2.83	90.75
1.35	96.08
0.43	99.39

465

y(mm)	x(mm)
0.60	0.00
1.66	5.40
2.72	10.79
3.87	21.58
4.68	32.37
4.85	43.17
4.99	48.56
4.68	53.96
4.35	64.75
3.56	75.54
2.73	86.34
1.38	91.73
0.00	99.39

619

y(mm)	x(mm)
0.27	0.00
1.38	3.82
2.17	7.97
3.41	16.27
4.34	24.57
5.09	32.87
5.55	41.17
5.72	49.47
5.48	57.77
5.04	66.07
4.40	74.37
3.43	82.67
2.22	90.97
1.53	95.12
0.71	99.27
0.00	102.01

679

y(mm)	x(mm)
0.00	0.00
1.64	6.20
2.60	12.39
4.03	24.78
4.99	37.18
5.16	43.37
5.11	49.57
5.11	55.76
4.85	61.96
3.93	74.35
2.41	86.74

624

y(mm)	x(mm)
0.89	0.00
1.76	6.38
2.67	12.76
3.45	25.53
3.84	38.29
3.91	51.06
3.52	63.82
2.85	76.58

492 cont.

5.58	18.64
7.65	27.96
8.53	37.28
9.09	46.60
9.49	55.92
9.54	79.22
8.84	83.88
7.06	93.20
6.17	97.86
5.81	99.40

493

y(mm)	x(mm)
2.77	0.00
3.45	4.61
4.35	9.22
5.11	18.43
5.63	27.65
6.10	36.86
6.56	46.08
6.64	55.30
5.92	64.51
5.05	73.73
3.50	82.94
2.08	92.16
0.00	99.40

682

y(mm)	x(mm)
0.00	0.00
2.20	6.31
4.03	12.62
6.96	25.24
8.56	37.85
8.98	44.16
9.06	50.47
9.00	56.78
8.85	63.09
7.70	75.71
5.59	88.33
4.31	94.64
3.32	99.18

494

y(mm)	x(mm)
4.50	0.00
5.74	2.99

494 cont.

6.09	5.97
6.68	8.96
7.92	17.91
8.82	26.87
9.17	35.82
9.27	44.78
9.09	53.73
8.31	62.69
7.17	71.64
5.63	80.60
3.37	89.55
2.51	92.54
1.65	95.52
0.34	98.51
0.00	99.40

572

y(mm)	x(mm)
0.00	0.00
1.23	4.88
2.45	11.13
4.55	23.63
5.15	29.88
5.60	36.13
6.04	48.63
5.95	54.88
5.82	61.13
4.97	73.63
4.31	79.88
3.21	86.13
1.93	92.38
1.42	95.00

499

y(mm)	x(mm)
0.00	0.00
0.37	4.50
1.30	13.50
2.03	22.50
2.77	31.50
3.42	40.50
3.13	49.50
2.69	58.51
2.04	67.51
1.52	76.51
0.69	85.51
0.09	90.01

621

y(mm)	x(mm)
0.00	0.00
1.92	4.13
3.44	8.26
6.02	16.52
7.18	24.79
7.95	33.05
8.14	41.31
8.62	49.57
8.54	57.83
8.12	66.10
7.18	74.36
5.76	82.62
4.04	90.88
2.92	95.01
1.39	99.76

681

y(mm)	x(mm)
0.34	0.00
2.17	6.25
3.30	12.49
4.15	18.74
5.11	24.98
5.80	31.23
6.42	37.48
6.72	43.72
6.90	49.97
6.71	56.21
6.32	62.46
5.64	68.71
4.87	74.95
4.16	81.20
2.95	87.44
1.60	93.69
0.00	98.81

579

y(mm)	x(mm)
0.00	0.00
0.84	4.88
1.62	14.64
2.28	24.40
2.74	34.15
3.05	43.91
3.00	53.67
2.71	63.43

579 cont.

2.08	73.19
1.07	82.95
0.31	87.83

580

y(mm)	x(mm)
0.00	0.00
0.88	4.85
2.07	14.56
3.24	24.27
3.80	33.97
3.87	43.68
3.76	53.39
3.30	63.09
2.72	72.80
1.94	82.50
1.26	87.36

730

y(mm)	x(mm)
0.77	0.00
2.11	4.97
2.84	9.93
4.45	19.86
5.60	27.79
6.45	39.72
6.59	44.69
6.58	49.65
6.57	54.62
6.47	59.58
5.70	69.51
4.78	79.44
4.12	84.41
3.54	89.37
2.59	94.34
0.00	99.55

476

y(mm)	x(mm)
1.56	0.00
2.29	5.05
3.50	10.11
5.12	20.21
5.92	30.32
6.13	40.42
5.98	50.53
5.54	60.64

476 cont.

4.48	70.74
3.37	80.85
1.45	90.95
0.00	99.39

590

y(mm)	x(mm)
0.00	0.00
0.89	6.33
2.04	19.00
2.39	25.33
2.58	31.67
3.02	44.33
3.04	50.67
2.97	57.00
2.73	63.33
2.60	69.66
2.22	76.00
1.65	82.33
1.18	86.57

593

y(mm)	x(mm)
0.42	0.00
1.17	6.60
2.28	19.80
2.75	26.40
3.01	33.00
3.14	46.21
3.10	52.81
2.87	59.41
2.21	72.61
1.70	79.21
0.97	85.81
0.00	92.41

594

y(mm)	x(mm)
3.02	0.00
3.58	6.60
4.04	19.80
4.08	26.40
4.08	33.00
3.94	39.60
3.78	52.81
3.47	59.41
2.75	72.61

594 cont.

1.96	79.21
1.10	85.81
0.00	92.41

473 cont.

1.73	86.54
.98	92.30
0.00	99.40

627

y(mm)	x(mm)
1.24	0.00
2.14	6.44
2.66	12.88
3.48	25.76
3.88	38.63
3.88	51.51
3.45	64.39
2.75	77.26
1.48	90.15
0.64	96.59
0.00	100.06

689

y(mm)	x(mm)
0.00	0.00
0.76	3.87
1.41	7.74
2.43	15.47
3.21	23.21
3.79	30.95
4.20	38.69
4.41	46.42
4.37	54.16
4.76	61.90
3.85	69.63
3.39	77.37
2.81	85.11

741 cont.

1.17	91.54
0.63	95.90
0.00	99.82

686

y(mm)	x(mm)
0.00	0.00
1.77	7.75
2.82	15.49
3.64	23.24
4.28	30.98
4.80	38.73
5.08	46.48
5.14	54.22
5.24	61.97
5.21	69.71
4.89	77.46
4.24	85.21
2.96	92.95
1.97	96.83
0.61	100.23

480

y(mm)	x(mm)
0.00	0.00
.86	5.00
1.77	10.01
2.84	20.01
3.76	30.02
4.18	40.02
4.60	50.03
4.41	60.03
4.00	70.04
3.15	80.04
1.99	90.05
.71	99.40

628

y(mm)	x(mm)
0.51	0.00
1.59	6.40
2.28	12.80
3.11	25.59
3.59	38.39
3.61	51.18
3.16	63.98
2.47	76.78
1.88	83.17
1.27	89.57
0.37	95.97
0.00	99.04

739

y(mm)	x(mm)
0.00	0.00
1.22	8.67
1.86	17.35
2.35	26.02
2.59	34.69
2.91	43.37
2.94	52.04
2.91	60.71
2.71	69.38
2.51	78.06
1.82	86.73
0.45	95.40

917

y(mm)	x(mm)
2.90	0.00
3.54	4.04
4.05	8.08
4.81	16.16
5.24	24.24
5.58	32.32
5.69	40.40
5.45	48.48
5.14	56.56
4.49	64.64
3.82	72.72
3.02	80.80
2.13	88.88
1.56	92.92
0.80	96.96
0.00	99.91

687

y(mm)	x(mm)
1.94	0.00
4.43	7.75
5.46	15.49
6.57	30.98
6.86	46.48
6.66	54.22
6.22	61.97
4.79	77.46
3.70	85.21
2.46	92.95
0.00	100.16

481

y(mm)	x(mm)
1.31	0.00
1.82	10.04
2.50	20.07
3.30	30.11
3.73	40.14
3.92	50.18
3.53	60.21
3.04	70.25
2.30	80.28
1.14	90.32
.46	95.34
0.00	99.40

628

y(mm)	x(mm)
0.56	0.00
1.34	3.87
1.89	7.74
2.63	15.47
3.20	23.21
3.65	30.95
3.90	38.69
1.02	46.42
3.94	54.16
3.78	61.90
3.41	69.63
2.88	77.37
2.21	85.11
1.23	92.84
0.00	99.27

739

y(mm)	x(mm)
0.00	0.00
1.22	8.67
1.86	17.35
2.35	26.02
2.59	34.69
2.91	43.37
2.94	52.04
2.91	60.71
2.71	69.38
2.51	78.06
1.82	86.73
0.45	95.40

918

y(mm)	x(mm)
0.00	0.00
0.80	4.04
1.20	8.08
1.99	16.16
2.53	24.24
2.92	32.32
3.22	40.40
3.45	48.48
3.55	52.52
3.49	56.56
3.40	64.64
3.22	72.72
2.92	80.80
2.40	88.88
2.01	92.92
1.45	96.96
0.87	99.95

473

y(mm)	x(mm)
.18	0.00
.73	5.77
1.33	11.54
2.16	23.08
2.64	34.61
2.92	46.15
2.94	57.69
2.83	69.23
2.31	80.77

626

y(mm)	x(mm)
2.91	0.00
3.97	6.44
4.62	12.88
5.54	25.76
5.91	38.63
5.74	51.51
4.88	64.39
3.76	77.27
2.03	90.15
0.71	96.59
0.00	99.55

741

y(mm)	x(mm)
0.39	0.00
1.06	4.36
1.73	8.72
2.36	17.44
2.75	26.15
2.99	34.87
3.08	43.59
3.05	52.31
2.84	61.03
2.54	69.74
2.15	78.46
1.59	87.18



Fig. 1: Four fressed 2" x 12" TET Charges Shot Simultaneously with No. 8 EB Caps in Parallel

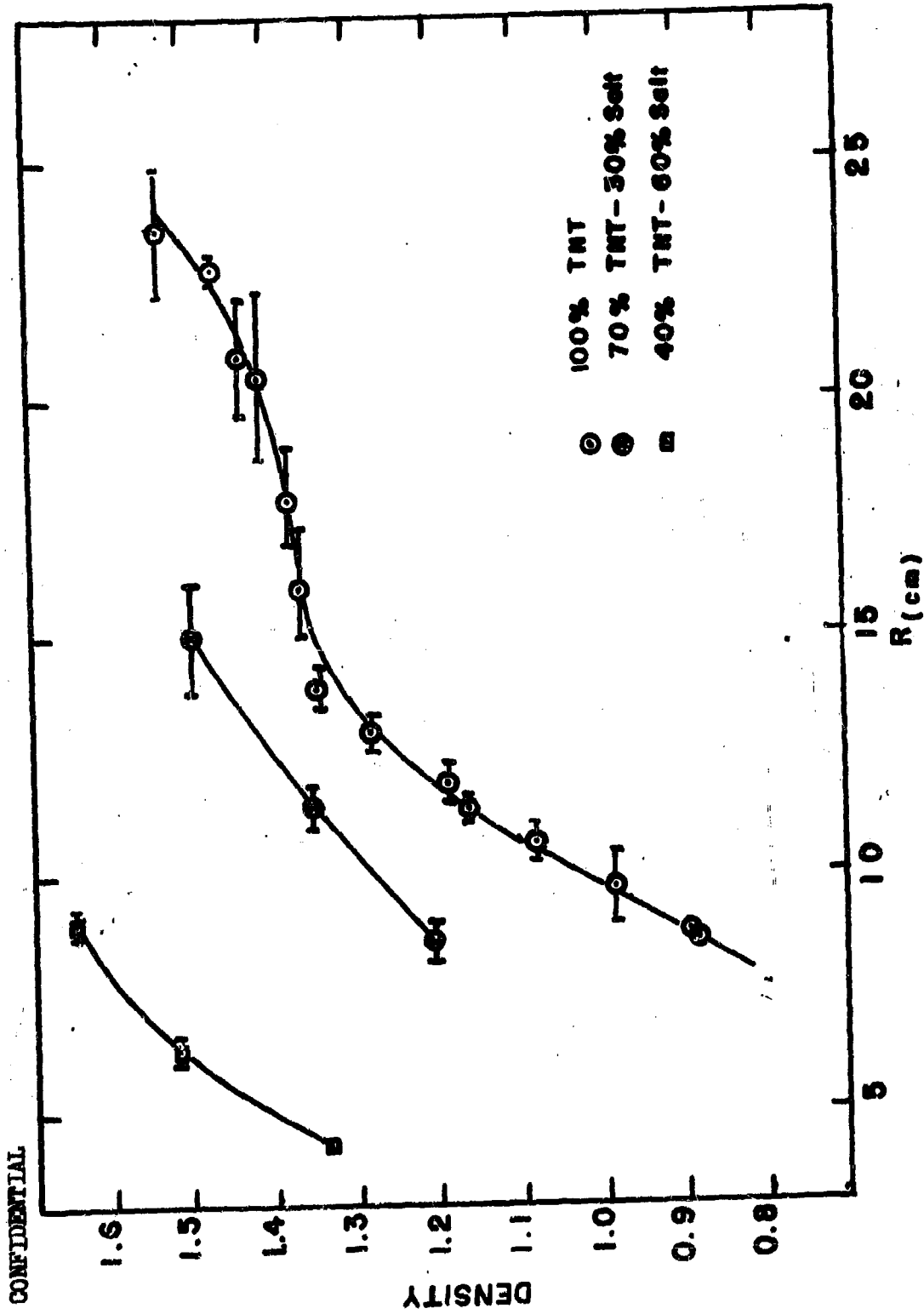


Fig. 2: Radius of Curvature-Density Curves for TNT and TNT-Salt
in 5.17 cm. Diameter Cylindrical Charges

CONFIDENTIAL

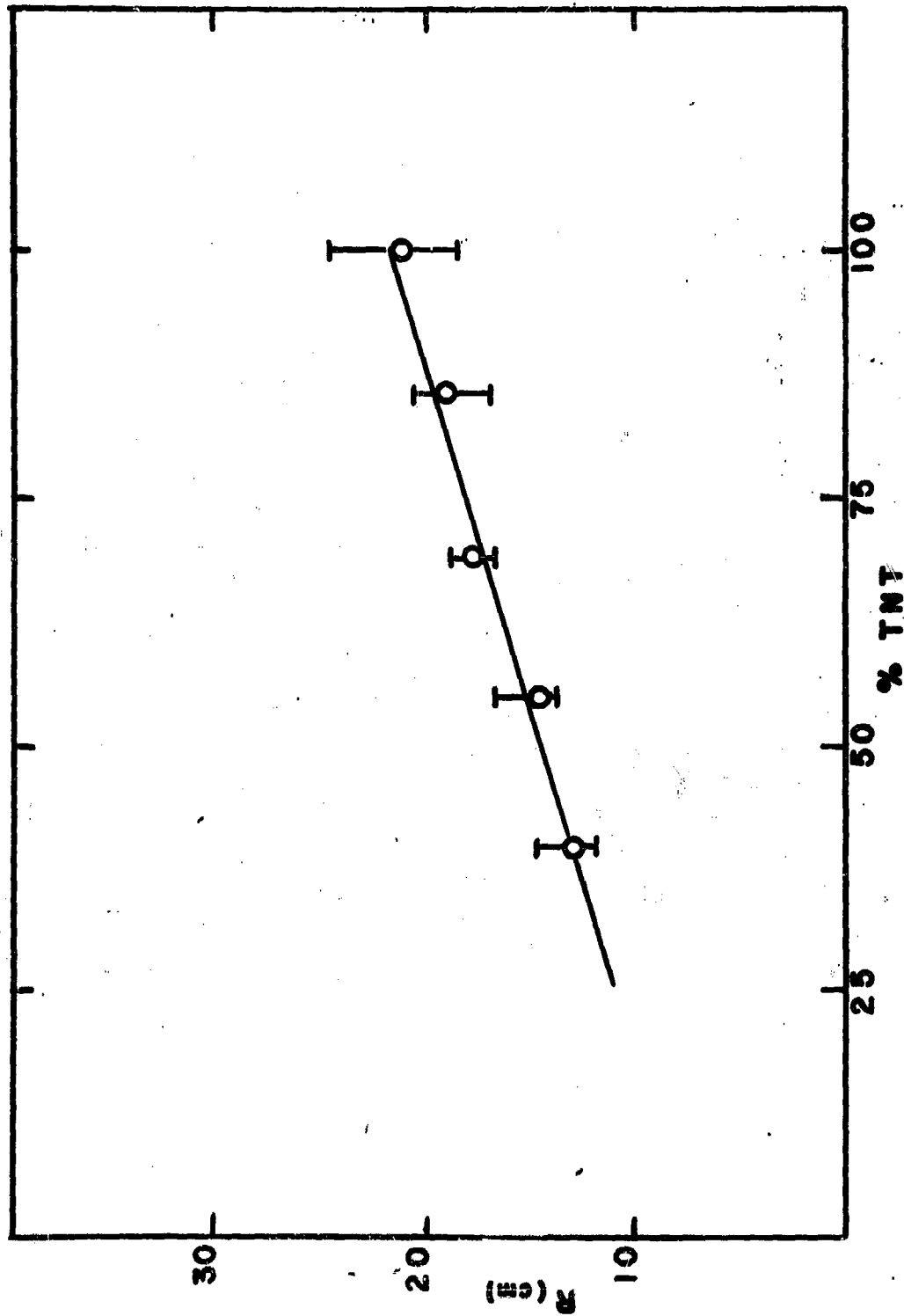


Fig. 3: Wave Shape-per cent TNT Curve for Vibrator-Packed TNT-Salt Mixtures in 9.94 cm. Diameter Cylindrical Charges

CONFIDENTIAL

CONFIDENTIAL

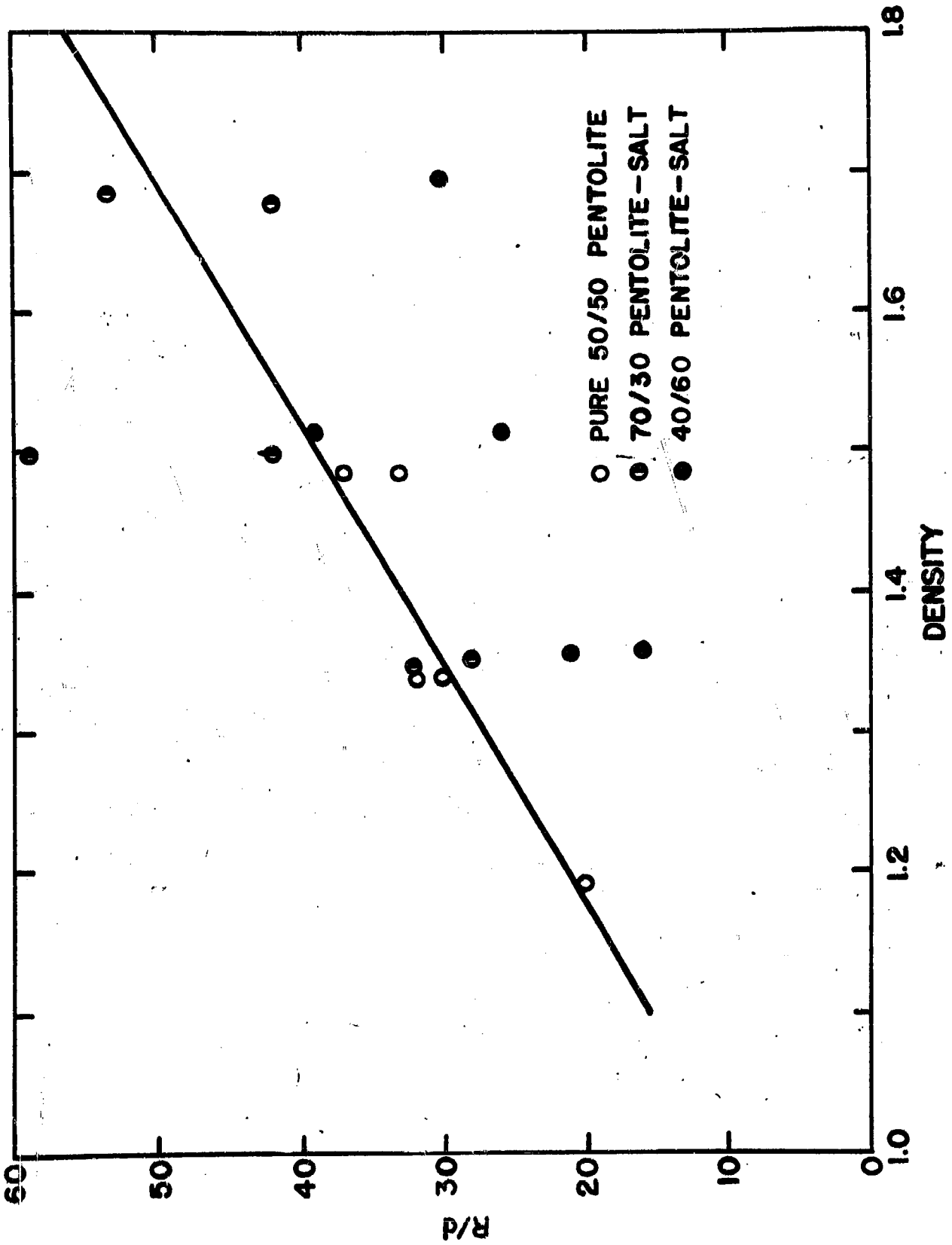


Fig. 4: R/d - Density for 50-50 Pentolite-Salt Mixtures in 5.17 cm. Cylindrical Charges

CONFIDENTIAL

CONFIDENTIAL

APPENDIX I

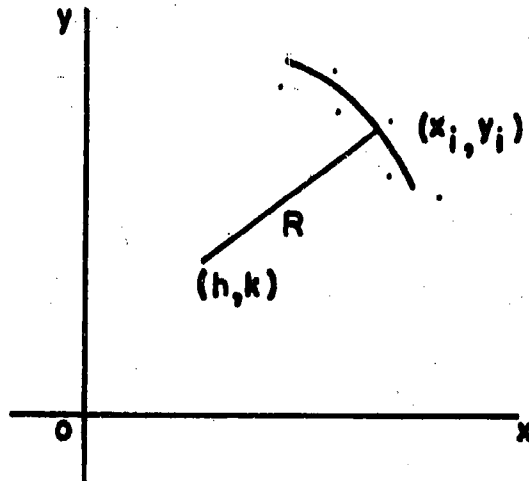
Best Fit to a Circular Arc

In the following paragraphs is given a method of obtaining a best fit to a circular arc of a set of points given in a cartesian coordinate system. The scheme is best adapted to the use of IBM or desk calculators. Suggestions are given to simplify calculations of a particular problem, and an illustration is included to indicate the procedure of application.

Consider an arbitrary plane cartesian coordinate system, with n points denoted by (x_1, y_1) . Let

$$(x - h)^2 + (y - k)^2 = R^2 \quad (1)$$

be the equation of a circle of radius R and center (h, k) . Consider also



the sum of the squared differences of the squared radius of the circle and each distance squared from each point to the center of the circle. That is

$$\delta = \sum_1^n ((x_1 - h)^2 + (y_1 - k)^2 - R^2)^2 \quad (2)$$

Differences of squared distances are considered to simplify the normal equations obtained by minimizing expression (2).

Differentiating δ partially with respect to h , k , and R , respectively, and simplifying the equations obtained by equating each expression to zero,

CONFIDENTIAL

$$\begin{aligned}\sum_1 ((x_1 - h)^2 + (y_1 - k)^2 - R^2) x_1 &= 0 \\ \sum_1 ((x_1 - h)^2 + (y_1 - k)^2 - R^2) y_1 &= 0 \\ \sum_1 ((x_1 - h)^2 + (y_1 - k)^2 - R^2) &= 0\end{aligned}\quad (3)$$

where it is assumed that $R \neq 0$. Or,

$$\begin{aligned}F_1 &= a_1^1 + a_1^2 h + a_1^3 h^2 + a_1^4 k + a_1^5 k^2 + a_1^6 R^2 \\ F_2 &= a_2^1 + a_2^2 h + a_2^3 h^2 + a_2^4 k + a_2^5 k^2 + a_2^6 R^2 \\ F_3 &= a_3^1 + a_3^2 h + a_3^3 h^2 + a_3^4 k + a_3^5 k^2 + a_3^6 R^2\end{aligned}\quad (4)$$

where F_1 , F_2 , and F_3 are respectively the three expressions of (3), and

$$\begin{aligned}a_1^1 &= \frac{\sum_1 (x_1^3 + x_1 y_1^2)}{\sum_1 x_1} & a_2^1 &= \frac{\sum_1^2 (x_1 y_1 + y_1^3)}{\sum_1 y_1} & a_3^1 &= \frac{\sum_1 (x_1^2 + y_1^2)}{n} \\ a_1^2 &= -\frac{2\sum_1 x_1^2}{\sum_1 x_1} & a_2^2 &= -\frac{2\sum_1 x_1 y_1}{\sum_1 y_1} & a_3^2 &= -\frac{2\sum_1 x_1}{n} \\ a_1^3 &= 1.0 & a_2^3 &= 1.0 & a_3^3 &= 1.0 \\ a_1^4 &= -\frac{2\sum_1 x_1 y_1}{\sum_1 x_1} & a_2^4 &= -\frac{2\sum_1 y_1^2}{\sum_1 y_1} & a_3^4 &= -\frac{2\sum_1 y_1}{n} \\ a_1^5 &= 1.0 & a_2^5 &= 1.0 & a_3^5 &= 1.0 \\ a_1^6 &= -1.0 & a_2^6 &= -1.0 & a_3^6 &= -1.0\end{aligned}\quad (5)$$

The coefficients of each equation are divided respectively by $\sum_1 x_1$, $\sum_1 y_1$, and n to simplify the solution of these equations.

These equations of (4) are non-linear in the unknowns h , k , and R . A method of solution by successive solution of a system of linear equations is easily given by the use of Taylor's expansion of F_1 , F_2 , and F_3 around an assumed set of values for the unknowns. Let h , k , and R be the values satisfying the equations, and 0h , 0k , and 0R a set of assumed

values. Then if

$$h = {}^0h + h' \quad k = {}^0k + k' \quad R = {}^0R + R'$$

and

$${}^0F_1^1 = a_1^2 + 2a_1^3 {}^0h \quad {}^0F_1^2 = a_1^4 + 2a_1^5 {}^0K \quad {}^0F_1^3 = 2a_1^6 {}^0R \quad (6)$$

neglecting second order terms and higher,

$$\begin{aligned} {}^0F_1^1 h' + {}^0F_1^2 k' + {}^0F_1^3 R' &= -{}^0F_1 \\ {}^0F_2^1 h' + {}^0F_2^2 k' + {}^0F_2^3 R' &= -{}^0F_2 \\ {}^0F_3^1 h' + {}^0F_3^2 k' + {}^0F_3^3 R' &= -{}^0F_3 \end{aligned} \quad (7)$$

Solving the system (7) for h' , k' , and R' , these corrections can be applied to the assumed values by use of (6) to give another set of approximations. The scheme is repeated until a satisfactory set of parameters is obtained.

Simple geometric considerations give the following first approximations to the desired parameters, providing that the set of points reasonably lie on a circular arc, and that the coordinate system is such that the chord connecting the two end points is approximately parallel to, say, the x-axis.

$${}^0h = \frac{x_1 + x_m}{2} \quad {}^0R = \frac{\bar{k}^2 + \bar{h}^2}{2\bar{k}} \quad {}^0k = y_m - {}^0R \quad (8)$$

where y_m is the maximum ordinate, and

$$\bar{h} = \frac{x_m - x_1}{2} \quad \bar{k} = y_m - \frac{y_1 + y_m}{2}$$

The data for the following illustration were taken from film no. 420. Computation was done on a desk calculator. A value of 27.182 cm. was obtained as the value of the radius of curvature. A previous graphical solution gave a value of 24.57 cm., which indicates an error of nearly 10 per cent.

Using the above suggestion to obtain a first approximation to the parameters, a second guess was made after substituting these values in the equations. The first iteration then gave the correct parameter values to four significant figures. A standard deviation computed from the value of the radius was found to be 0.0173 cm.

Illustration No. 420

x (cm.)	y (cm.)
0.000	0.0066
0.630	0.2148
1.260	0.3238
1.890	0.4229
2.520	0.5303
3.150	0.6046
3.780	0.6905
4.410	0.7219
5.040	0.7517
5.670	0.7814
6.300	0.7814
6.930	0.7764
7.560	0.7566
8.190	0.7302
8.820	0.6938
9.450	0.6377
10.080	0.5369
10.710	0.4246
11.340	0.2974
11.970	0.1635
12.600	0.0000

n = 21

$$\Sigma x_1 = 132.3$$

$$\Sigma x_1^2 = 11,39.1$$

$$\Sigma x_1^3 = 10,961.98$$

$$\Sigma y_1 = 10.847$$

$$\Sigma y_1^2 = 6.94097$$

$$\Sigma y_1^3 = 4.71978$$

$$\Sigma x_1 y_1 = 68.2863$$

$$\Sigma x_1^2 y_1 = 0.515965$$

$$\Sigma x_1 y_1^2 = 43.7363$$

11005.716	-2278.2	132.3	-136.573	132.3	-132.3
520.685	-136.573	10.847	-13.8819	10.847	-10.847
1146.04	-264.6	21.0	-21.694	21.0	-21.0

CONFIDENTIAL

-42-

83.188	-17.219	1.0	-1.0323	1.0	-1.0
48.003	-12.591	1.0	-1.2798	1.0	-1.0
54.573	-12.600	1.0	-1.0330	1.0	-1.0

6.3	39.69	-21.06	443.52	447.42	(21.85)
-----	-------	--------	--------	--------	---------

2.74

2.25

1.42

6.3	39.69	-23.8	566.44	605.16	(24.6)
-----	-------	-------	--------	--------	--------

-4.619	-48.6323	-49.2	-0.247
--------	----------	-------	--------

0.009	-48.8798	-49.2	-0.109
-------	----------	-------	--------

0.000	-48.6330	-49.2	-0.748
-------	----------	-------	--------

-4.619	10.528751	10.651656	0.053474
--------	-----------	-----------	----------

0.009	-48.974559	1.006560	0.002235
-------	------------	----------	----------

0.000	-48.633000	-0.247968	2.598175
-------	------------	-----------	----------

-0.108856	-2.592853	2.578175	
-----------	-----------	----------	--

6.191	38.328	-26.393	696.590	738.644	(27.178)
-------	--------	---------	---------	---------	----------

-4.8370	-53.8183	-54.3560	-0.1047
---------	----------	----------	---------

-0.2090	-54.0658	-54.3560	-0.1039
---------	----------	----------	---------

-0.2180	-53.8190	-54.3560	-0.1044
---------	----------	----------	---------

-4.8370	11.126380	11.237543	0.021645
---------	-----------	-----------	----------

-0.2090	-51.740387	1.005159	0.001920
---------	------------	----------	----------

-0.2180	-51.393449	-0.247629	0.004062
---------	------------	-----------	----------

0.000065	-0.002163	0.004062	
----------	-----------	----------	--

CONFIDENTIAL

CONFIDENTIAL

-43-

6.191065 38.329 -26.39516 696.704 738.864 (27.18206)

-0.00077

-0.00083

-0.00078

h = 6.191

k = -26.395

R = 27.182

R² = 738.864

$(x_1 - h)^2 + (y_1 - k)^2$	$((x_1 - h)^2 + (y_1 - k)^2)^{1/2}$	$(x_1 - h)^2 + (y_1 - k)^2 - R^2$	$((x_1 - h)^2 + (y_1 - k)^2) - R^2$ b_1
738.513	27.176	-0.351	-0.006
739.006	27.185	0.142	0.003
738.209	27.170	-0.655	-0.012
737.698	27.161	-1.166	-0.021
738.448	27.174	-0.416	-0.008
738.226	27.171	-0.638	-0.011
739.432	27.192	0.568	0.010
738.498	27.175	-0.366	-0.007
738.268	27.172	-0.596	-0.010
738.828	27.181	-0.036	-0.001
738.568	27.177	-0.296	-0.005
738.831	27.182	-0.033	0.000
739.083	27.186	0.219	0.004
739.772	27.199	0.908	0.017
740.715	27.216	1.851	0.034
741.388	27.229	4.524	0.047
740.451	27.211	1.587	0.029
739.712	27.198	0.848	0.016
738.996	27.185	0.132	0.003
738.750	27.180	-0.114	-0.002
737.771	27.162	-1.093	-0.020

s.d. = $(\sum b_1^2 / 21)^{1/2} = 0.0173$

s.d. is the standard deviation taken from R = 27.182.

CONFIDENTIAL

CONFIDENTIAL

-44-

Film No. 420, for the above illustration, shows the wave shape of an amatol charge. This film is not included in any of the studies of the body of this report. Even though the graphical and the analytical methods give radii of curvature which differ by ten per cent, the valuable conclusion can be drawn that standard deviation of only 0.0173 cm. for an $R = 27.182$ cm. indicates that an arc of a circle can reasonably be used to fit the wave shape.

Two curves from this report were also checked by the above method. They were No. 984 and No. 987 found in Table I. By the graphical method, R 's of 23.1 cm. and 24.8 cm. were respectively obtained. By the analytical method, corresponding R 's of 24.3 cm. and 24.6 were obtained. The difference is five per cent for No. 984 and less than one per cent for No. 987. These results indicate that the graphical method yield values that are satisfactory for wave shape.

CONFIDENTIAL

CONFIDENTIAL

Distribution List

Commanding Officer
Office of Naval Research, Branch Office
150 Causeway Street
Boston, Massachusetts Copy No. 1

Office of Naval Research, Branch Office
The John Crerar Library Building
Tenth Floor, 86 East Randolph Street
Chicago 1, Illinois Copy No. 2

Commanding Officer
Office of Naval Research, Branch Office
346 Broadway
New York, New York Copy No. 3

Director
Office of Naval Research, Branch Office
1000 Geary Street
San Francisco 9, California Copies 4,5

Commanding Officer
Office of Naval Research, Branch Office
1030 North Green Street
Pasadena 1, California Copy No. 6

Officer in Charge
Office of Naval Research, Branch Office
Navy Number 100, Fleet Post Office
New York, New York

Director, Naval Research Laboratory
Washington 25, D. C.
Attention: Technical Information Officer
Copy No. 8

Research and Development Board
Pentagon, Room 3D1041
Washington 25, D. C.
Attention: Technical Reference Section
Copy No. 9

Chief of Naval Research
Office of Naval Research
Washington 25, D. C.
Attention: Chemistry Branch
Copies 10-18

Commanding General
Wright Air Development Center
Attention: Dr. L. A. Wood
Wright-Patterson Air Force Base
Ohio Copy No. 19

Dr. A. Weissler
Department of the Army
Office of the Chief of Ordnance
Washington 25, D. C.
Attention: ORDTB-PS Copy No. 20

Research and Development Group
Logistics Division, General Staff
Department of the Army
Washington 25, D. C.
Attention: Dr. W. T. Read
Scientific Advisor Copy No. 21

Director, Naval Research Laboratory
Washington 25, D. C.
Attention: Chemistry Division
Copies 22, 23

Chief of the Bureau of Ships
Navy Department
Washington 25, D. C.
Attention: Code 340 Copies 24, 25

Chief of the Bureau of Aeronautics
Navy Department
Washington 25, D. C.
Attention: Code TD-4 Copies 26, 27

Chief of the Bureau of Ordnance
Navy Department
Washington 25, D. C.
Attention: Code Re2d Copy No. 28
Attention: Code Re2C (Dr. Brownard) Copy No. 29

US Naval Radiological Defense Laboratory
San Francisco 24, California
Attention: Technical Library
Copy No. 30

CONFIDENTIAL

Distribution List (cont'd)

Dr. John S. Rinehart
Michelson Laboratory
Naval Ordnance Test Station (Inyokern)
China Lake, California Copy No. 52

Commanding Officer
Picatinny Arsenal
Dover, New Jersey Copy No. 53

Arthur D. Little, Inc.
30 Memorial Drive
Cambridge 42, Massachusetts
Attention: Dr. W. C. Lothrop Copy No. 54

Commander
Naval Ordnance Test Station (Inyokern)
China Lake, California
Attention: Technical Library Copy No. 55

Dr. A. G. Horney
Office of Scientific Research
R and D Command USAF
Box 1395
Baltimore, Maryland Copy No. 56

Our Files Copies 57-65